

Submitted to The Astronomical Journal, 5 December 2002

## Is the Redshift Clustering of Long-Duration Gamma-Ray Bursts Significant?

J. S. Bloom<sup>1,2</sup>

<sup>1</sup> *Harvard Society of Fellows, 78 Mount Auburn Street, Cambridge, MA 02138 USA*

<sup>2</sup> *Harvard-Smithsonian Center for Astrophysics, MC 20, 60 Garden Street, Cambridge, MA 02138, USA*

### ABSTRACT

The 26 long-duration gamma-ray bursts (GRBs) with known redshifts form a distinct cosmological set, selected differently than other cosmological probes such as quasars and galaxies. Since the progenitors are now believed to be connected with active star-formation and since burst emission penetrates dust, one hope is that with a uniformly-selected sample, the large-scale redshift distribution of GRBs can help constrain the star-formation history of the Universe. However, we show that strong observational biases in ground-based redshift discovery hamper a clean determination of the large-scale GRB rate and hence the connection of GRBs to the star formation history. We then focus on the properties of the small-scale (clustering) distribution of GRB redshifts. When corrected for heliocentric motion relative to the local Hubble flow, the observed redshifts appear to show a propensity for clustering: eight of 26 GRBs occurred within a recession velocity difference of  $1000 \text{ km s}^{-1}$  of another GRB. That is, four pairs of GRBs occurred within  $30 h_{65}^{-1} \text{ Myr}$  in cosmic time, despite being causally separated on the sky. We investigate the significance of this clustering using a simulation that accounts for at least some of the strong observational and intrinsic biases in redshift discovery. Comparison of the numbers of close redshift pairs expected from the simulation with that observed shows no significant small-scale clustering excess in the present sample; however, the four close pairs occur only in about twenty percent of the simulated datasets (the precise significance of the clustering is dependent upon the modeled biases). We conclude with some impetuses and suggestions for future precise GRB redshift measurements.

*Subject headings:* cosmology: miscellaneous — cosmology: observations — gamma rays: bursts

### 1. Introduction

A growing body of evidence suggests that long-duration GRBs arise from the death of massive stars. If true, the large-scale redshift distribution of GRBs should trace the star-formation history

of the Universe (Totani 1997; Wijers et al. 1998; Lamb & Reichart 2000; Porciani & Madau 2001; Bromm & Loeb 2002). And, as explosive and transient events detectable to high redshift, GRBs clearly offer a probe of the Universe that is distinct from other lighthouses (Loeb 2002). Already, GRBs have helped shed light on the nature of damped Lyman  $\alpha$  absorbers (e.g., Fynbo et al. 2002) and the nature of the faint end of the luminosity function of galaxies at moderate redshifts (e.g., Djorgovski et al. 2001b).

As a redshift sample selected from an apparent isotropic population and from hosts spanning the breadth of the galaxy luminosity function, GRBs have the potential to provide a unique census of the redshift distribution of matter in the Universe. Not only can the large-scale distribution of GRBs help constrain the star-formation rate (SFR), but, in a manner complementary to pencil-beam surveys and magnitude-limited galaxy and quasar surveys, the small-scale distribution can help test hypotheses and observational suggestions about clustering and periodicity of sources in redshift space.

Given the penetrative powers of GRBs through dust, several studies have attempted to compare the large-scale redshift distribution of GRBs with the SFR obtained by other means (Schaefer et al. 2001; Lloyd-Ronning et al. 2002a; Stern et al. 2002; Norris 2002). Such studies focused on using the prompt  $\gamma$ -ray properties of BATSE bursts, calibrated with some measured GRB redshifts, to determine the bursting rate. With so few actual redshifts measured, each of which were measured under different observational constraints, the task of distinguishing different SFR scenarios from the sparsely sampled GRB rate is considerably challenging. Indeed we show herein, that when the observational biases in redshift determination are taken into account, several proposed forms for the universal SFR cannot be distinguished.

Investigation of the small-scale distribution of GRBs has not been presented thus far. Of particular interest is whether the clustering properties in redshift space are significant in light of the observational biases and the intrinsic redshift distribution. Do GRBs occur at preferred redshifts? There is enough historical, albeit controversial, evidence to warrant an investigation of the significance of special redshifts in the Universe using GRBs. Broadhurst et al. (1990), for instance, found evidence for periodicity of clustering of redshifts on  $128 h^{-1}$  Mpc scales in two pencil-beam surveys. While excess power on these scales has not been definitively confirmed in higher-redshift studies (e.g., with the 2dF redshift survey: Hawkins et al. 2002; although see Gal & Djorgovski 1997 and Duari et al. 1992) the Broadhurst et al. result may be statistically significant in comparison with  $N$ -body simulations (Yoshida et al. 2001). But, as Yoshida et al. emphasize, large clusters in a galaxy sample tend to accentuate the appearance of excess power at certain scales<sup>1</sup>. A GRB sample does not suffer such a bias since bursts occur in regions of space that are

---

<sup>1</sup>Excess power on such  $128 h^{-1}$  Mpc scales could be an imprint of a primordial density fluctuation (Dekel et al. 1992). As a statistical measure, if this interpretation is true, then the same redshifts with over-densities would not reoccur in surveys that sample different directions on the sky. However, specific special redshifts would be preferred if the observed power arises by more exotic means. For example, oscillations of the scalar potential (Morikawa 1991)

gravitationally (and causally) disconnected.

The focus of this paper is on the small-scale (clustering) distribution of GRB redshifts. In addition we examine the large-scale distribution of GRB redshifts, and note the difficulty in determining the global GRB rate due to the small sample and strong observational biases. In §2 we present the GRB redshift sample for 26 bursts, corrected for the heliocentric motion through the local Hubble flow and construct an observationally-motivated probability distribution for redshift discovery. In §3, we compare the large-scale distribution of GRB redshifts with that expected from the observing biases and an intrinsic rate distribution. After showing the insensitivity of the present sample to distinguishing various SFRs, and under the *ansatz* that GRBs *should* trace the SFR, we fix a model for redshift discovery probability that adequately reproduces the universal SFRs. Using this distribution, we then test the significance of the number of observed pairs of GRBs with small recession velocity differences. We conclude with a discussion about the importance and usefulness of conducting precise redshift measurements for future GRBs.

## 2. The Redshift Sample

Table 1 presents a summary of the sky location and observed redshifts associated with 26 cosmological GRBs, in order of increasing redshift. The highest observed redshift system derived using absorption or emission features with the highest reported accuracy is given in column seven. The line features used to measure the reported redshift are given in column six. Absorption-line redshifts, which place a strict lower limit to the actual GRB redshift, are found when a spectrum of the afterglow is absorbed by metal-line systems along the line of sight. Emission-line redshifts are derived from spectroscopy of the galaxy associated with the GRB position, either found promptly, superimposed with the spectrum of the transient afterglow (e.g., 980703; Djorgovski et al. 1998), or at later times, when the afterglow light has faded. Nineteen sources in the sample have measured emission-line redshifts, and 12 have absorption-line redshifts. The uncertainty in the redshift measurements are usually provided in the literature, but where none were provided we assumed an error of 10 percent in the least significant digit reported.

Since we are interested in testing the observed rate and redshift distribution of GRBs against different models for star-formation and small-scale clustering, we now discuss the observational biases in GRB detection, localization, and finally, redshift determination.

---

or the gravitational constant (Salgado et al. 1996) induce an oscillation in the Hubble constant versus cosmic time. The result is an apparent clustering of sources in redshift space at epochs where the expansion temporarily slows.

## 2.1. Biases in GRB Detection

If GRBs arise in collimated emission, then the relativistic Doppler beaming allows for detection of a GRB only if the detector lies in the direction of the cone of emission. By studying the opening angles of those GRBs which have been detected, it is reckoned that only about one in every five hundred GRBs are detectable at (i.e., pointed toward) Earth due to beaming (Frail et al. 2001).

Of those bursts that are beamed toward Earth, only those that reach a certain critical flux level will be detected by the triggering algorithms of a given satellite. The typical threshold for on-board detection in the BATSE catalog is a peak flux of a  $0.3 \text{ photon cm}^{-2} \text{ s}^{-1}$  (in 't Zand & Fenimore 1994; Pendleton et al. 1998). In finding that the total energy release in GRBs is approximately constant, Frail et al. (2001) showed that bursts that are more highly collimated appear to be intrinsically brighter (in flux/fluence per unit solid angle). Thus, for a scenario where GRBs are jetted and release about the same amount of electromagnetic energy, brighter bursts tend to be *more distant*. As a clear illustration of this, note that the peak flux of the highest redshift burst, GRB 000131 ( $z = 4.5$ ), was at the top 5% of the entire BATSE catalogue (Andersen et al. 2000).

This somewhat counterintuitive trend implies that the brightest GRBs can be detected to extremely high redshifts, certainly beyond the age of reionization ( $z \sim 7\text{--}10$ ). More important for the present study is that Malmquist bias should play little role in diminishing the observed burst rate at high-redshift: bursts significantly fainter (by up to  $\sim 10^{-3}$ ) than GRB 000131 could have been detected at similar redshifts.

Using the prompt high-energy properties, irrespective of individual burst redshifts, it has been shown that the brightness distribution of GRBs is consistent with a broad range of star-formation rates and luminosity functions (e.g., Loredó & Wasserman 1998; Kommers et al. 2000; Schmidt 2001; Stern et al. 2002). Using distance indicators calibrated from a sub-set of the bursts with known redshift, Lloyd-Ronning et al. (2002b) claimed that the GRB rate increases monotonically at least out to  $z \approx 10$ . In our opinion, this suggestion points more to the pitfalls of extrapolating GRB distance indicators beyond the redshift range in which they were calibrated, than revealing concrete properties of the high-redshift bursting rate density. Another approach to constrain the burst rate, which we attempt herein, is to use only those bursts with actual measured redshifts.

## 2.2. Biases in Afterglow Localization

For those GRBs that are triggered and rapidly localized using the prompt X-rays or  $\gamma$ -rays, the observing community tries to determine a sub-arcsec position and ultimately associate a redshift via host or absorption-line spectroscopy. This is accomplished by first identifying a transient afterglow.

Three major biases are important for afterglow discovery. First, GRBs will be preferentially localized if they occur at a time and place in the sky where ground- or space-based telescopes can rapidly observe the prompt burst position with large enough fields-of-view. Second, only GRB

afterglows with brightnesses above a given threshold for the particular afterglow-discovery observations will be localized. Last, only GRB afterglows that are not heavily extinguished by dust obscuration will be first localized at optical wavelengths. Clearly, radio and X-ray afterglow discoveries do not suffer this third bias. The existence of a population of dark bursts (Djorgovski et al. 2001a; Piro et al. 2002), those bursts without detectable optical afterglow emission, is clearly a result of all three biases. (The current dark burst debate revolves around the relative importance of dust versus observational biases in the manifestation of dark bursts (Berger et al. 2002; Fynbo et al. 2001).)

Since, for now, GRBs with redshifts are preferentially those that were first localized at optical wavelengths (all but 970828, 980329, and 000210 were first localized at optical wavelengths), it seems appropriate to suppose that a population of optically-localized GRBs should trace a star-formation rate derived from other optically-selected samples; Porciani & Madau (2001) have provided a parameterized version of a SFR based upon the un-dust corrected Hubble Deep Field measurements (model SF1); in this model the SFR drops beyond  $z \sim 2$ . In future GRB redshift samples of bursts that are first localized at radio, X-ray or even infrared wavelengths, the expectation is that the observed rate will more closely trace the true (high mass) SFR in the universe.

### 2.3. Biases in Redshifts Determination

For those GRBs that are triggered and localized, most are followed up spectroscopically. If an absorption or emission-line redshift is found, it is of interest to know the relationship between this and the true GRB redshift. A definitive measure of burst redshifts would need to connect the bursting location with some stationary gas local to the GRB, resulting in a detection of transient features. To date, no transient absorption or emission features at optical wavelengths features have been associated with a GRB afterglow. Transient features, consistent with (later-time) optical spectroscopic redshift measurements, have been seen in a prompt burst spectrum (Amati et al. 2000; Le Floc’h et al. 2002) and a handful of X-ray afterglow spectra (e.g., Piro et al. 1999, 2000). At present, the uncertainties in these X-ray-derived redshifts are orders of magnitude larger than those found typically at optical wavelengths. Perhaps more important, redshifts derived purely from X-ray spectroscopy are contaminated from an unknown (potentially relativistic) outflow speed of the emitting or absorbing material; thus, precise measurements of the systematic redshift of GRB progenitors are best determined using the UV and optical features of host HII regions and/or intervening host clouds.

If a GRB occurs in intergalactic space, with no afterglow absorption due to local gas, then the observed redshift would be systematically lower than the true redshift. However, to date, the nature of the highest  $z$  absorption lines, suggests the presence of gas columns and abundances not typically associated with tenuous outflow gas halos of galaxies. Specifically, the equivalent widths of the highest redshift absorption systems in GRB afterglows are significantly larger than in systems seen through quasar lines-of-sight (e.g., Salamanca et al. 2002). This is naturally understood in the context of the prevailing progenitor model, namely that long-duration bursts arise from the death

of massive stars and, owing to the rapid evolution of massive stars, GRB explosion locations should be in or near relatively dense regions of active star-formation. Thus, GRBs should reside in or near the region that gives rise to the gas absorption. Consistent with this picture is the observation that well-localized GRBs, a subset of which comprises the present sample, have been observationally connected to the location of the light of the putative host galaxies (Bloom et al. 2002).

The probability of a spurious (spatial) association of an afterglow with its putative host has been shown to be small ( $\lesssim 10^{-2}$ ) for most bursts. In fact in a sample of 20 GRBs with arcsecond localizations, statistically, at most a few spatial associations could have been spurious (Bloom et al. 2002). Therefore, from the location argument, GRB redshifts determined from emission line spectroscopy of the hosts are likely to be close to the true systematic velocities of the progenitor; at most, we would expect a velocity offset on the order of a few hundred  $\text{km s}^{-1}$  from the motion of the progenitor system about its host. Likewise, unless the afterglow light pierces some high-velocity outflowing material, absorption-line redshifts should also provide an accurate measure of the true GRB redshift. Perhaps most convincing that measured redshifts are closely related to the real systemic redshifts, is that of the five GRBs with both emission and absorption line spectroscopy, the highest redshift absorption system is always found to be consistent with the emission-line redshift of the host.

#### 2.4. Correcting the measured redshifts for heliocentric motion relative to the local Hubble frame

One striking feature of the current redshift sample is the small apparent redshift differences, on the order of a thousand  $\text{km s}^{-1}$ , between some bursts from different sky locations and apparently random trigger dates (differences of 6 months to 5 years). (Unlike in pencil-beam surveys the proximity in redshift can have nothing to do with systems, such as galaxies in clusters, that are in causal contact.) These small velocity differences are comparable to the velocity of the Solar System through the local Hubble frame, and so a correction for this systematic motion is warranted. Such motion was measured by the angular dependence of temperature variations in the Cosmic Microwave Background (CMB) with the COBE satellite (Smoot et al. 1991; Fixsen et al. 1994). This measured velocity ( $V_{\odot} = 365 \pm 18 \text{ km s}^{-1}$ ) and direction (toward Galactic coordinates  $l = 264.4 \pm 0.3 \text{ deg}$ ,  $b = 48.4 \pm 0.5 \text{ deg}$ ; Fixsen et al. 1994) are due to vector sum of the heliocentric motion about the Galactic center, the peculiar motion of the Milky Way in the Local Group and the Local Group in-fall. We assume that all reported redshifts have been corrected to the heliocentric redshifts; this correction is at most of order tens of  $\text{km s}^{-1}$  and so this assumption is relatively unimportant.

In order to remove this systematic bias from a measured redshift  $z$ , we find the angle ( $\theta_{\text{CMB}}$ ) between the GRB position and the heliocentric motion through the CMB; we then find the projected heliocentric velocity toward the GRB as  $v_{\odot,\text{proj}} = V_{\odot} \cos \theta_{\text{CMB}}$ . If  $uc$  is the uncorrected apparent recession velocity of a distant source, then, from the definition of redshift and the formula for

relativistic velocity addition, the corrected redshift in the local Hubble frame (lhf) is found from:

$$(1 + z_{\text{lhf}})^2 = \frac{1 + uv_{\odot,\text{proj}}/c + u + v_{\odot,\text{proj}}/c}{1 + uv_{\odot,\text{proj}}/c - u - v_{\odot,\text{proj}}/c}, \quad (1)$$

with the uncorrected apparent recession velocity as,

$$u = \frac{(1 + z)^2 - 1}{(1 + z)^2 + 1}. \quad (2)$$

The calculated values of  $z_{\text{lhf}}$  are given in column eight of Table 1. The associated uncertainties are derived by error analysis of equation 1, assuming that the errors on  $V_{\odot}$  and  $\theta_{\text{CMB}}$  are uncorrelated and noting that the fractional error on  $\theta_{\text{CMB}}$  is significantly smaller than the fractional error on  $V_{\odot}$ . As seen in Table 1, for all but the most accurately measured redshifts, this correction adds negligibly to the fractional error of the redshift.

### 3. Results

Table 2 shows the absolute difference in redshift and recession velocity of each burst matched with the burst that is closest in apparent recession velocity. Figure 1 shows this distribution of “nearest neighbor” apparent recession velocity differences versus redshift. The smallest groupings occur around redshift of unity, where the density of known GRB redshifts is highest. Four pairs are closer than  $\sim 1000 \text{ km s}^{-1}$  ( $0.0034 c$ ) in redshift space<sup>2</sup>, and the largest velocity difference is between the two highest redshift bursts ( $|\Delta v| = 0.22 c$ ).

Interestingly, the velocity differences of the four closest burst pairs (at redshifts  $z = 0.692$ ,  $0.844$ ,  $0.961$ , and  $2.035$ ) are less than the velocity dispersion of a large cluster of galaxies—and so, given the unknown peculiar velocity of the GRB hosts and the progenitor system within the hosts, these close burst pairs are consistent with having occurred at the same cosmic time. Even assuming no peculiar velocities of GRB progenitors relative to their local Hubble flow, eight of 26 GRBs occurred within  $30 h_{65}^{-1} \text{ Myr}$  of another GRB. This was determined by computing the look-back times between the four close pairs and assuming a cosmology with  $H_0 = 65 \text{ km s}^{-1} \text{ Mpc}^{-1}$ ,  $\Omega_{\Lambda} = 0.7$  and  $\Omega_{\text{m}} = 0.3$ . This cosmology is assumed throughout the paper where needed.

#### 3.1. Simplistic probability calculation

How significant is this proximity in cosmic time? The bursts listed in Table 1 have been detected with recession velocities in the range  $v_{\text{low}} = 0.30 c$  (GRB 011121) to  $v_{\text{high}} = 0.94 c$  (GRB 000131).

---

<sup>2</sup>Of the eight bursts in the close four pairs, six redshifts were determined via emission lines from the putative host galaxies. One redshift (GRB 000926) was one with absorption spectroscopy only and another redshift (GRB 000301C) was found with both emission and absorption spectroscopy.

In an ensemble of  $n$  bursts, assuming uniform probability of a GRB occurring and being detected between  $v_{\text{low}}$  and  $v_{\text{high}}$ , the probability that given pair of successive bursts are not as close as a distance  $\Delta v_c$  is  $P = \exp(-n(v_{\text{high}} - v_{\text{low}})/\Delta v_c)$ . Therefore, the probability that at least one close pair exists in the ensemble, is,

$$P(1) = 1 - P^{n-1} \quad (3)$$

For  $\Delta v_c = 1000 \text{ km s}^{-1}$  and  $n = 26$ , the probability of at least one close pair with  $\Delta v \leq 1000 \text{ km s}^{-1}$  is 0.967. The probability of at least one close pair with at most the smallest velocity difference in the observed GRB sample ( $\Delta v_c = 259 \text{ km s}^{-1}$ ) is 0.585. Both these probabilities thus indicate that there is nothing particularly unusual about the occurrence of *at least one* close pair in the current sample.

In general, the probability that exactly  $k$  pairs are close can be approximated as,

$$P(k) \approx \left[ \frac{n(v_{\text{high}} - v_{\text{low}})}{\Delta v_c} \right]^k \frac{P^{n-1} \times n!}{(n-k)! k!} \quad (4)$$

For the present sample, there are  $k = 4$  close pairs. Using this simplistic calculation we therefore expect four pairs to occur by random chance in 18.6% of samples. We have verified this approximation by a Monte Carlo simulation, selecting  $n$  bursts uniformly over the range  $[v_{\text{low}}, v_{\text{high}}]$ ; however, this approximation breaks down for large velocity differences as it does not account for relativistic velocity subtraction between successive bursts in velocity space.

### 3.2. Probability calculation with a model distribution

The above probability estimate does not take into account some important observational and endemic biases. First, the rate of GRBs is not uniform in redshift or recession velocity space. Instead, we expect GRBs to trace (or at least approximate) the star-formation rate (Totani 1997; Wijers et al. 1998), so that the peak of bursting activity should occur around  $z \sim 1 - 2$ . This will make close velocity pairs more likely at redshifts near unity. Second, the chance that a burst will be *localized* well enough to follow-up with spectrometers is not uniform in redshift. Instead, this chance depends, for optical localizations, sensitively on the native dust obscuration of the afterglow (see §2.2). Third, observing conditions and instrumentation play a strong role in determining whether the redshift of a GRB can be detected at that redshift. Most important, emission lines and absorption lines falling outside the broadband spectral coverage hamper the ability to detect redshifts (this may be an explanation for why no redshifts have been detected for 980519, 980326, and 980329). Even if a redshifted line falls within the spectral range, the presence of night sky lines make detection of redshifts at certain wavelengths more unlikely. Fourth, instrumental sensitivity varies across the spectral range and from instrument to instrument, night to night, and airmass to airmass.

Since we wish to know how the observed redshift sample compares with that expected given the above considerations we construct a toy probability model,  $P(z)$ , giving the differential prob-

ability that a burst at redshift  $z$  could ultimately yield a redshift measurement. We construct a global (rather than individual) distribution, neglecting the instrumental sensitivity differences from burst to burst and the non-negligible chance that a redshift will be incorrectly assigned even after the detection of one or more spectral features. We use several parametrized versions of the star formation rate (SFR) from Porciani & Madau (2001). The overall shape of the distribution,  $P_G(z)$ , is then proportional to the number of bursts per unit redshift per unit observer time; that is,  $P_G(z)$  is proportional to the co-moving volume element and the co-moving SFR ( $\rho_{\text{SFR}}$ ) versus redshift:

$$P_G(z) \propto \frac{dN}{dt dz} \propto \frac{\rho_{\text{SFR}} dV}{1+z dz} \propto \left( \frac{\exp(3.4 z)}{\exp(3.8 z) + 45} \right) \times \frac{d_L^2(z)}{(1+z)^3 \sqrt{\Omega_m(1+z)^3 + \Omega_k(1+z)^2 + \Omega_\Lambda}}, \quad (5)$$

following eqs. [2]–[4] in Porciani & Madau (2001). Here  $d_L(z)$  is the luminosity distance and  $\Omega_m + \Omega_k + \Omega_\Lambda = 1$ . The factor of  $(1+z)$  in the denominator accounts for the time dilation of the co-moving GRB rate. Following the discussion in §2.2, we have nominally chosen the un-dust corrected SFR from Porciani & Madau (2001) (SF1). We also explore the two other models for  $P_G(z)$  in Porciani & Madau (2001). In our model we do not take into account any biases related to the distance of the source in localization (in §2.2 we argued that there should be little bias in triggering based on distance). However, because of the observed anti-correlation between jet opening angles and prompt emission fluence (Frail et al. 2001), and the theoretical correlation between prompt burst emission and afterglow luminosity (Panaitescu et al. 2001), aside from dust obscuration, the afterglow from *triggered* GRBs that originate from higher redshift GRBs should not be significantly dimmer at the same observer time (see also Ciardi & Loeb 2000; Lamb & Reichart 2000).

Nevertheless, if there is any dependence of triggering/localization on  $d_L$ , we can try to account for such using a probability function related to luminosity distance,  $P_L(z)$ . There is also a clear effect of distance upon redshift discovery: once a burst afterglow is localized and a spectrum is acquired, the detectability of emission features is diminished with increasing luminosity distance (nominally as  $d_L^{-2}$ ). Systematically, only GRB hosts with higher rates of unobscured star formation will be detectable at higher redshifts for a given integration time. For a given afterglow brightness, the distance bias does not exist for absorption-redshift GRBs as long as the particular redshifted line is observable in the spectrum. To try to account for these elusive effects, we take the probability of redshift discovery due to distance [ $P_L(z)$ ] as unity from  $z = 0$  to  $z_l$ , decreasing with  $d_L$  to some power  $L$ . Nominally we take the values of  $z_l = 1$  and  $L = -2$  but allow these quantity to vary in our modeling (see §3.3).

Using the observability of emission and absorption lines in the spectral range and in the presence of night skylines, we construct a relative probability of redshift detection,  $P_S(z)$ . We take the spectrum range as 3800–9800 Å and assume a redshifted line is not observable if it falls within a wavelength that is half the instrumental resolution of a strong sky line listed in Osterbrock & Martel (1992). Here, we assume the instrumental resolution of 5 Å (dispersion of  $\sim 2.5$  Å/pixel).

Based upon Table 1, we assume that a redshift can be obtained unambiguously with the detection of at least one of four star-formation emission features: Ly  $\alpha$   $\lambda$ 1216 Å, [O II]  $\lambda\lambda$ 3727 Å, H $\alpha$  6563 Å, and [O III]  $\lambda\lambda$  4959, 5008 Å. Also based on Table 1, for redshifts based upon absorption features only, we require that at least three of the following lines are detectable: Fe II  $\lambda$ 2344.2 Å, Fe II  $\lambda$  2374.5 Å, Fe II  $\lambda$  2382.8 Å, Fe II  $\lambda$  2586.7 Å, Fe II  $\lambda$  2600 Å, Mg II  $\lambda\lambda$  2796.4, 2803.5 Å, Mg I  $\lambda$  2853.0 Å. If no redshifted star formation line nor prominent absorption line is observable at a given redshift,  $z_0$ , then we set  $P_S(z_0) = 0$ . Even if a line is observable, it may be too weak in emission or too low in equivalent width to be detected. Therefore with less and less lines observable at a given  $z$ , the value of  $P_S(z)$  should be diminished.

Figure 3 shows our toy model for  $P_S(z)$ , based upon the above considerations. We stress that this is a toy model for ground-based optical spectroscopy. Different instruments will provide free-spectral ranges that differ from our nominal range (3800–9800 Å). The resolution of each instrument also will also particularly affect the observability of faint, narrow emission/absorption features in the presence of sky lines. A moderate-resolution spectrograph ( $R \gtrsim 10000$ ) should allow for feature detection closer in wavelength to a sky line; even features which partially overlap a skyline could be detectable (e.g., Bloom et al. 2003).

The resultant relative probability distribution of detecting an optical redshift for a triggered GRB is constructed as  $P(z) = P_G(z) \times P_S(z) \times P_L(z)$  and is depicted in Figure 4. The relative probability distribution was calculated in bins of  $\delta z = 0.001$ . As can be seen in the normalized cumulative distributions shown in Figure 2, the overall shape of the cumulative distributions are largely unaffected by the sky lines. The most pronounced feature in  $P(z)$  is the drop in detection probability from  $z \approx 1.5 - 2$ , due to the inaccessibility of strong emission lines in the optical bandpass. The relative probability for detection of bursts at the redshift of GRB 980425 ( $z = 0.0088$ ) is exceedingly small and thus serves to emphasize the distinction between GRB 980425 and the other long-duration GRBs with known redshift (e.g., Galama et al. 1998; Bloom et al. 1998; Schmidt 2000; Porciani & Madau 2001). As such, we have not included GRB 980425 in our analysis.

### 3.3. Consistency of the Large-Scale GRB Distribution with a Variety of SFR Models

As shown in Figure 2, the large-scale shape of the observed redshift distribution is adequately described by the model for  $L = -2$ , with the KS probability that the observed deviations are consistent with a random selection from the model of  $P_{KS} = 0.64$  (SF1), 0.51 (SF2), and 0.32 (SF3). Models where no account for the observational bias of detecting emission lines from high-redshift GRB hosts ( $L = 0$ ) are clearly ruled out. While there are small differences in the KS probability between various models for the star-formation rate, such models cannot be statistically distinguished by the current sample of GRBs with known redshifts. However, given the low KS probabilities for  $L = 0$ , the data do support the notion that the observational biases of detecting emission lines from high-redshift GRB hosts must be taken in account. Note that a fairly large

range of  $L$  values ( $\approx -1$  to  $-3$  for SF1) yields a KS consistency with the data.

How sensitive are these results to our toy model for  $P_G(z)$  and  $P_L(z)$ ? Changing the value of  $z_l$  we still get acceptable (but lower) KS statistics for  $L = -2$ :  $P_{KS} = 0.20$  ( $z_l = 0.5$ ; SF1),  $0.22$  ( $z_l = 1.25$ ; SF1),  $0.04$  ( $z_l = 1.5$ ; SF1). With  $z_l > 4.5$ , the  $L = -2$  case is effectively equivalent to the  $L = 0$  case ( $P_{KS} = 0.003$  for  $z_l = 5$ ; SF1). By removing the effect of the sky lines and limited free-spectral range in redshift determination, the KS statistics are still acceptable, albeit with lower values of the KS statistic:  $P_{KS} = 0.37$  (SF1),  $0.19$  (SF2),  $0.10$  (SF3).

### 3.4. Testing the Small-Scale GRB Redshift Distribution

Assuming that GRBs *do* trace the global star-formation rate we fix the form of  $P_L(z)$  that gives a reasonable agreement with all three SF models. From here, we can test the significance of the small-scale clustering properties. To do so, we produce a Monte Carlo realization as sets of GRB redshifts drawn from the probability for redshift detection  $P(z)$  for each SFR model. We simulated 5000 iterations of sets of GRB redshifts. For each iteration, 26 bursts were selected uniformly from  $[0,1]$  and then mapped to redshift using the cumulative and normalized distribution of  $P(z)$ , interpolating between bins to increase the resolution.

We thought of no obvious existing statistic to compare the small-scale redshift structure of the observed distribution with the Monte Carlo set. However, since one feature is the existence of such close redshift pairs we can ask how often such numbers of pairs are found in the distribution. Table 3 summarizes the results of the comparison. Column two lists the number of observed GRBs within an apparent recession velocity of  $|\Delta v|$  of another GRB. Columns three, four and five give the probability of such occurrences in the simulated distributions for the three different GRB rates,  $P_G(z)$ . Following the table, the simulation predicts that at least two bursts (one pair) should occur by random chance in 53% of real world samples for the smallest observed velocity difference. This is close to the probability obtained in our simplistic calculation (59%) in §3.1. For  $\Delta v$  values near  $1000 \text{ km s}^{-1}$ , the probability drops to  $\approx 19\%$  before rising again at large velocity offsets. Therefore, despite the apparent close pairings in redshift space, we find no significant small-scale redshift clustering in the present sample.

Note, however, this comparison only references 2-point correlations. Following column eight of Table 1 and column 6 of Table 2, there are two groupings of three bursts within  $2500 \text{ km s}^{-1}$  (at  $z = 0.69$  and  $z = 0.84$ ). Using the Monte Carlo set, the probability of getting 2 groupings of three bursts within  $2500 \text{ km s}^{-1}$  is  $0.24$  (SF1),  $0.17$  (SF2), and  $0.13$  (SF3). Again, the present sample shows no evidence for significant multi-burst clustering.

With the advent of *Swift*<sup>3</sup>, it is not unreasonable to expect upwards of one hundred new GRB

---

<sup>3</sup><http://www.swift.psu.edu/>

redshifts within the next several years. As the density of redshifts increases, the number of close redshift pairs (and triples) will certainly increase. Commensurately, for an expanded sample to yield significant clustering results, the number of close pairs must increase. Using the present models, as a function of bursts in a sample, we predict the required number of observed close pairs in order to be considered a significant excess above a random sample. Figure 5 depicts the results. For the present sample, approximately 1 (2) more close pairs would be needed with velocity differences less than  $1000 \text{ km s}^{-1}$ , for the clustering results to be considered significant at the 0.05 (0.01) level. From the Figure, we see that in a sample of 50 GRB redshifts, there is a 5% random chance of getting 5 close pairs within about  $250 \text{ km s}^{-1}$ . If 6 or 7 more pairs are found, this would be considered a significant result.

#### 4. Conclusions

We have demonstrated, via a KS test, that the large-scale distribution of observed long-duration GRB redshifts is compatible with having been drawn from a reasonable model for the detection probability of burst redshifts. This supports the suggestion, based upon  $\gamma$ -ray properties, that the rate of GRBs rises rapidly out to redshifts of order unity (cf. Schmidt 2000; Lloyd-Ronning et al. 2002a; Stern et al. 2002). To our knowledge, this is the first investigation to claim this using only the observed GRB redshifts and a model for the observational and intrinsic selection function for GRB redshift discovery.

The data are relatively insensitive to various forms of the underlying star-formation for a given set of redshift selection functions  $P_S(z)$  and  $P_L(z)$ . We have shown that by not considering the biases of ground-based optical spectroscopy in redshift determination (i.e., setting  $P_S(z) = 1$ ) the large-scale redshift distributions are still consistent with the SFR expectations, although at a lower significance. (Without the presence of sky-lines, a derivation of the functional form of  $P_S(z)$  will be significantly more tractable with redshifts obtained from space-based spectroscopy, such as from *Swift*.) The large-scale rate results are much more sensitive to  $P_L(z)$ , which is unfortunately the most difficult of the relevant probabilities to determine *ab initio*; in general  $P_L(z)$  should be constructed on a case-by-case basis, including any biases of distance upon triggering, localization probabilities, and redshift determination. There are certain psychological elements in the redshift determination (e.g., integrating longer until a redshift is found) that make this component particularly difficult to model. It is clear, since the large-scale KS probability drops precipitously for  $z_l \gtrsim 1.25$ , that there must be some strong diminution of the detection rate of redshifts at larger distances.

Given these difficulties, since we cannot test which star-formation rate GRBs trace best, we use the notion that GRBs *should* trace the universal SFR as a point of departure. That is, we fix a functional form of  $P(z)$  that provides a reasonable agreement with the expectations for the GRB rate on a large scale. Under this assumption ( $L = -2$  and  $z_l = 1$ ), we test the significance of the apparent small-scale clustering. As can be seen in Table 3, there does not appear to be any

significant small-scale clustering of GRBs in redshift space when compared with the Monte Carlo set; however, the observed number of bursts paired with  $|\Delta v| \lesssim 1000 \text{ km s}^{-1}$  occurs in only one out of five iterations.

The small-scale comparison in Table 3 is rather conservative, however. The only obvious *a posteriori* injection to the comparison is in choosing the velocity bins based upon the observed dataset. We have not required close pairs in the comparison set to fall within a certain redshift range, say  $z = [0.65, 2.05]$ , nor have we required that the close pairs in the comparison sets be spaced by at least  $\delta z = 0.1$  (as observed). Any such restrictions would tend to increase the significance of the observed small-scale clustering. However, without some *a priori* hypothesis that the particular redshifts and spacings in the observed datasets are of interest, further restrictions are unwarranted.

In the context of cosmologies with oscillating Hubble “constants” (see §1) some *a priori* preference for special redshifts may indeed exist. For example, we might expect that the most massive clusters of galaxies would reside at redshifts where the Hubble constant loiters at a local minimum. One of the most, if not the most massive clusters known, with the highest observed X-ray temperature and high velocity dispersion of member galaxies ( $\sigma > 1100 \text{ km s}^{-1}$ ), is MS 1054–03 (Neumann & Arnaud 2000; van Dokkum et al. 2000). Correcting the systemic redshift reported in van Dokkum et al. (2000) to the local Hubble frame (following §2.4), the redshift of the cluster is  $z_{\text{hf}} = 0.8337 \pm 0.0007$ . This is just  $177 \pm 125 \text{ km s}^{-1}$  from the redshift of GRB 970508 yet the cluster and the GRB site are separated by  $\Delta\theta = 88.4^\circ$  on the sky. Further, the redshift of MS 1054–03 is 1456 and 1872  $\text{km s}^{-1}$  from GRB 990705 and GRB 000210 (respectively), less than two times the velocity dispersion of the cluster itself. Using our Monte Carlo simulation with  $P_G(z) \propto \text{SF1}$ , the probability that three bursts out of 26 would fall within  $2000 \text{ km s}^{-1}$  of  $z = 0.8337$  by random chance is 0.035. Since the association with a massive cluster was chosen *a posteriori* we do not claim this to be a significant result, but it should be of interest to test the association of new GRB redshifts with other massive clusters at moderate to high redshifts.

The existence and expectation of several close groupings in redshift space holds some practical implications for observations of future GRBs. First, precise redshift determinations via moderate-resolution optical spectroscopy ( $R \gtrsim 1000$ ) will continue to be important even though approximate redshifts, using GRB distance-indicators (such as the Lag-Luminosity or Variability relations), may someday be used reliably to constrain the overall large-scale redshift distribution. Second, new future close redshift groupings will enable efficient detailed narrow-band imaging studies of multiple GRB hosts, such as the study of GRB 000926 and GRB 000301C (Fynbo et al. 2002).

We end by noting the curious absence of detected GRB redshifts in the redshift range between  $z \approx 2.3 - 3.2$ , where a relatively clean window for Lyman  $\alpha$  emission detection exists at optical wavelengths (see fig. 1). One explanation for this is that redshift discovery via Ly  $\alpha$  emission should be fruitless for about half of high redshift GRBs, since the average equivalent width of Ly  $\alpha$  for Lyman Break Galaxies beyond  $z \sim 3$  is near zero (K. Adelberger, personal communication); the absence of bursts in this range could simply be due to the low number of GRBs followed-up with

sufficiently small delay to detect Lyman  $\alpha$  in absorption at optical wavelengths. In this respect, the uniformity and sheer rate of redshift discovery with *Swift*, should be most enlightening.

## REFERENCES

- Amati, L. *et al.* 2000, *Science*, 290, 953
- Andersen, M. I. *et al.* 2000, *A&A*, 364, L54
- Barth, A. J. *et al.* 2003, *ApJ (Letters)*, 584, L47
- Berger, E. *et al.* 2002, *ApJ*, 581, 981
- Bloom, J. S., Berger, E., Kulkarni, S. R., Djorgovski, S. G., and Frail, D. A. 2003, *AJ*, in press
- Bloom, J. S., Djorgovski, S. G., and Kulkarni, S. R. 2001, *ApJ*, 554, 678
- Bloom, J. S., Djorgovski, S. G., Kulkarni, S. R., and Frail, D. A. 1998, *ApJ (Letters)*, 507, L25
- Bloom, J. S., Kulkarni, S. R., and Djorgovski, S. G. 2002, *AJ*, 123, 1111
- Bloom, J. S., Kulkarni, S. R., Harrison, F., Prince, T., Phinney, E. S., and Frail, D. A. 1998, *ApJ (Letters)*, 506, L105
- Broadhurst, T. J., Ellis, R. S., Koo, D. C., and Szalay, A. S. 1990, *Nature*, 343, 726
- Bromm, V. and Loeb, A. 2002, *ApJ*, 575, 111
- Castro, S. *et al.* 2001, GCN notice 999
- Castro, S. M., Diercks, A., Djorgovski, S. G., Kulkarni, S. R., Galama, T. J., Bloom, J. S., Harrison, F. A., and Frail, D. A. 2000a, GCN notice 605
- Castro, S. M. *et al.* 2000b, GCN notice 851
- Ciardi, B. and Loeb, A. 2000, *ApJ*, 540, 687
- Dekel, A., Blumenthal, G. R., Primack, J. R., and Stanhill, D. 1992, *MNRAS*, 257, 715
- Djorgovski, S. G., Bloom, J. S., and Kulkarni, S. R. 2000, *ApJ Lett.*, accepted; astro-ph/0008029
- Djorgovski, S. G., Diercks, A., Bloom, J. S., Kulkarni, S. R., Filippenko, A. V., Hillenbrand, L. A., and Carpenter, J. 1999, GCN notice 481
- Djorgovski, S. G., Frail, D. A., Kulkarni, S. R., Bloom, J. S., Odewahn, S. C., and Diercks, A. 2001a, *ApJ*, 562, 654

- Djorgovski, S. G. *et al.* 2001b, in Gamma-Ray Bursts in the Afterglow Era, Proceedings of the International workshop held in Rome, CNR headquarters, 17–20 October, 2000, ed. E. Costa, F. Frontera, & J. Hjorth (Berlin Heidelberg: Springer), 218
- Djorgovski, S. G., Kulkarni, S. R., Bloom, J. S., Goodrich, R., Frail, D. A., Piro, L., and Palazzi, E. 1998, *ApJ (Letters)*, 508, L17
- Duari, D., Gupta, P. D., and Narlikar, J. V. 1992, *ApJ*, 384, 35
- Fixsen, D. J. *et al.* 1994, *ApJ*, 420, 445
- Frail, D. A. *et al.* 2001, *ApJ (Letters)*, 562, L55
- Fynbo, J. P. U. *et al.* 2001, *A&A*, 369, 373
- . 2002, *A&A*, 388, 425
- Gal, R. and Djorgovski, S. G. 1997, in ASP Conf. Ser. 114: Young Galaxies and QSO Absorption-Line Systems, 79
- Galama, T. J. *et al.* 1998, *Nature*, 395, 670
- Garnavich, P. M. *et al.* 2003, *ApJ*, 582, 924
- Hawkins, E., Maddox, S. J., and Merrifield, M. R. 2002, *MNRAS*, 336, L13
- Holland, S. T. *et al.* 2002, *AJ*, 124, 639
- in 't Zand, J. J. M. and Fenimore, E. E. 1994, in AIP Conf. Proc. 307: Gamma-Ray Bursts, 692
- Kommers, J. M., Lewin, W. H. G., Kouveliotou, C., van Paradijs, J., Pendleton, G. N., Meegan, C. A., and Fishman, G. J. 2000, *ApJ*, 533, 696
- Kulkarni, S. R. *et al.* 1998, *Nature*, 393, 35
- . 1999, *Nature*, 398, 389
- Lamb, D. Q. and Reichart, D. E. 2000, *ApJ*, 536, 1
- Le Floc'h, E. *et al.* 2002, astro-ph/0211250
- Lloyd-Ronning, N. M., Fryer, C. L., and Ramirez-Ruiz, E. 2002a, *ApJ*, 574, 554
- . 2002b, *ApJ*, 574, 554
- Loeb, A. 2002, in Lighthouses of the Universe: The Most Luminous Celestial Objects and Their Use for Cosmology Proceedings of the MPA/ESO, 137
- Loredo, T. J. and Wasserman, I. M. 1998, *ApJ*, 502, 75

- Matheson, T. *et al.* 2002, ApJ Letters, accepted
- Morikawa, M. 1991, ApJ, 369, 20
- Neumann, D. M. and Arnaud, M. 2000, ApJ, 542, 35
- Norris, J. P. 2002, ApJ, 579, 386
- Osterbrock, D. E. and Martel, A. 1992, PASP, 104, 76
- Panaiteanu, A., Kumar, P., and Narayan, R. 2001, ApJ (*Letters*), 561, L171
- Pendleton, G. N., Hakkila, J., and Meegan, C. A. 1998, in Gamma Ray Bursts: 4th Huntsville Symposium, ed. C. A. Meegan, R. Preece, & T. Koshut, Vol. 428 (Woodbury, New York: AIP), 899–903
- Piro, L. *et al.* 1999, ApJ (*Letters*), 514, L73
- . 2002, ApJ, 577, 680
- . 2000, Science, 290, 955
- Porciani, C. and Madau, P. 2001, ApJ, 548, 522
- Price, P. A. *et al.* 2002a, ApJ, 573, 85
- . 2002b, ApJ (*Letters*), 571, L121
- . 2002c, submitted to Astrophysical Journal Letters
- Salamanca, I., Vreeswijk, P. M., Kaper, L., Rol, E., van den Heuvel, E. P. J., Tanvir, N., and Ellison, S. 2002, in Lighthouses of the Universe: The Most Luminous Celestial Objects and Their Use for Cosmology Proceedings of the MPA/ESO, 197
- Salgado, M., Sudarsky, D., and Quevedo, H. 1996, Phys. Rev. D, 53, 6771
- Schaefer, B. E., Deng, M., and Band, D. L. 2001, ApJ (*Letters*), 563, L123
- Schmidt, M. 2000, in AIP Conf. Proc. 526: Gamma-ray Bursts, 5th Huntsville Symposium, 58
- Schmidt, M. 2001, ApJ (*Letters*), 559, L79
- Smoot, G. F. *et al.* 1991, ApJ (*Letters*), 371, L1
- Steidel, C. C., Adelberger, K. L., Giavalisco, M., Dickinson, M., and Pettini, M. 1999, ApJ, 519, 1
- Stern, B. E., Tikhomirova, Y., and Svensson, R. 2002, ApJ, 573, 75
- Totani, T. 1997, ApJ (*Letters*), 486, L71

van Dokkum, P. G., Franx, M., Fabricant, D., Illingworth, G. D., and Kelson, D. D. 2000, *ApJ*, 541, 95

Vreeswijk, P. M. *et al.* 2001, *ApJ*, 546, 672

Vreeswijk, P. M. *et al.* 1999, GCN notice 496

Wijers, R. A. M. J., Bloom, J. S., Bagla, J., and Natarajan, P. 1998, *MNRAS*, 294, L17

Yoshida, N. *et al.* 2001, *MNRAS*, 325, 803

The author thanks D. Frail and P. van Dokkum for helpful suggestions in improving the paper and gratefully acknowledges discussions with K. Adelberger at several stages of this project. The anonymous referee is acknowledged and thanked for their insightful comments and suggestions. The author is supported by a Junior Fellowship to the Harvard Society of Fellows and by a generous research grant from the Harvard-Smithsonian Center for Astrophysics.

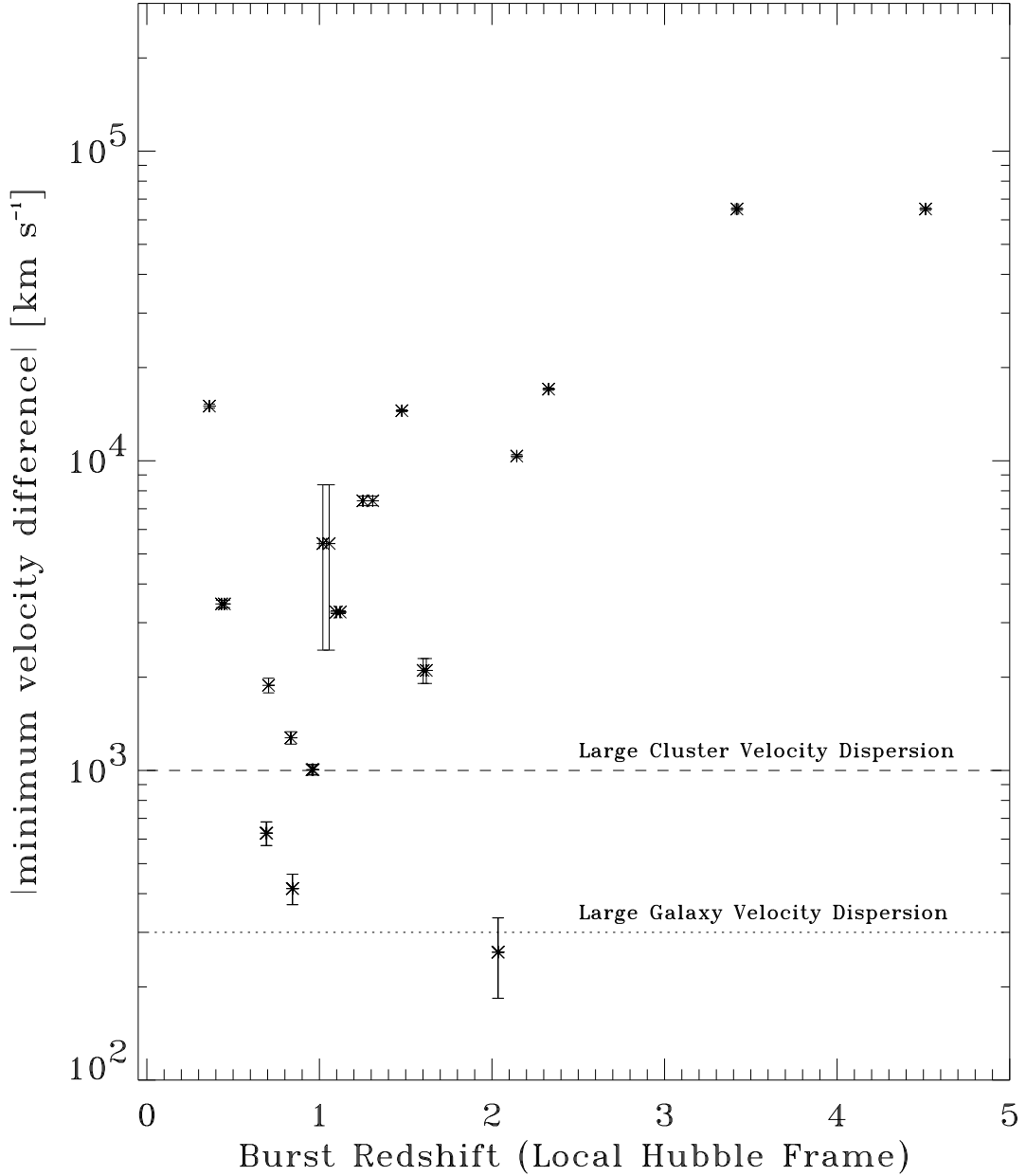


Fig. 1.— The distribution of recession velocity differences between nearest redshift pairs, following Table 2. The redshifts have been correction for the heliocentric motion through the local Hubble frame. Duari et al. 1992 performed a similar correction for quasar redshifts but only accounted for the heliocentric motion in the Galaxy. Representative velocity dispersions of galaxies and clusters are indicated with the dashed and dotted lines. There are 4 pairs of bursts which are separated by  $\lesssim 1000 \text{ km s}^{-1}$ .

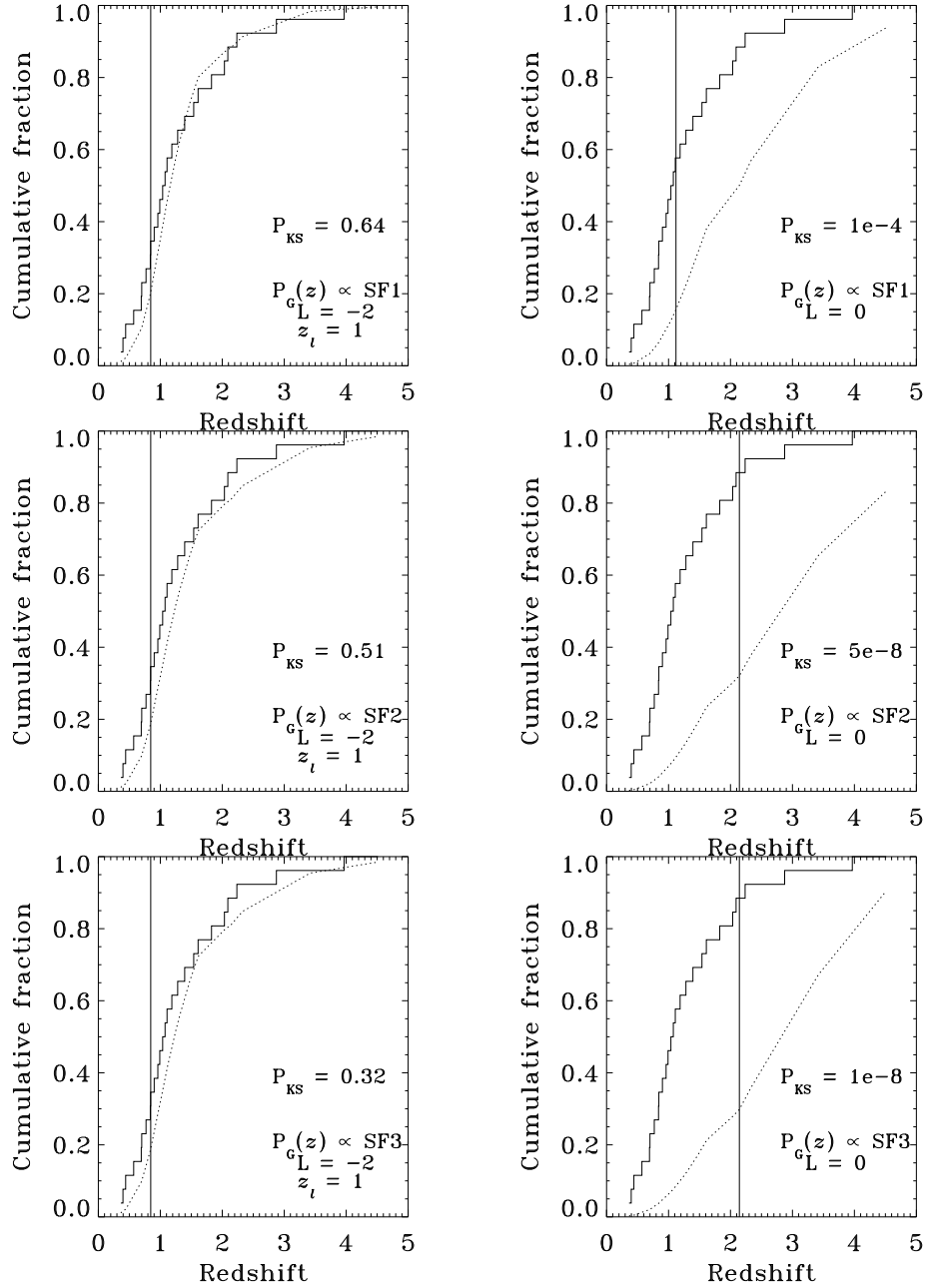


Fig. 2.— Comparison of the large-scale redshift distribution (solid cumulative line) with various models for redshift detection. Models (shown as dotted lines) that do not correct any observational biases in measuring high redshifts ( $L = 0$ ) are clearly ruled out, but very different models for the true rate, when including a simple model for the high redshift bias ( $L = -2$ ,  $z_l \lesssim 1.25$ ), are all allowed by the data. The Kolmogorov-Smirnov (KS) probabilities are given for six model comparisons, with the redshift of maximum deviation from the model noted with a vertical line. Clearly, the universal SFR cannot be *inferred* from the current sample. Here we have used GRB rate models that follow different parameterizations of the SFR (following Porciani & Madau 2001). SF1 is the so-called Madau rate, where the GRB rate falls beyond redshift of unity. SF2 is a dust-corrected form of the Madau rate that levels off beyond redshift of unity (e.g., Steidel et al. 1999). SF3 is a rate which continues to increase beyond  $z \approx 1.5$ .

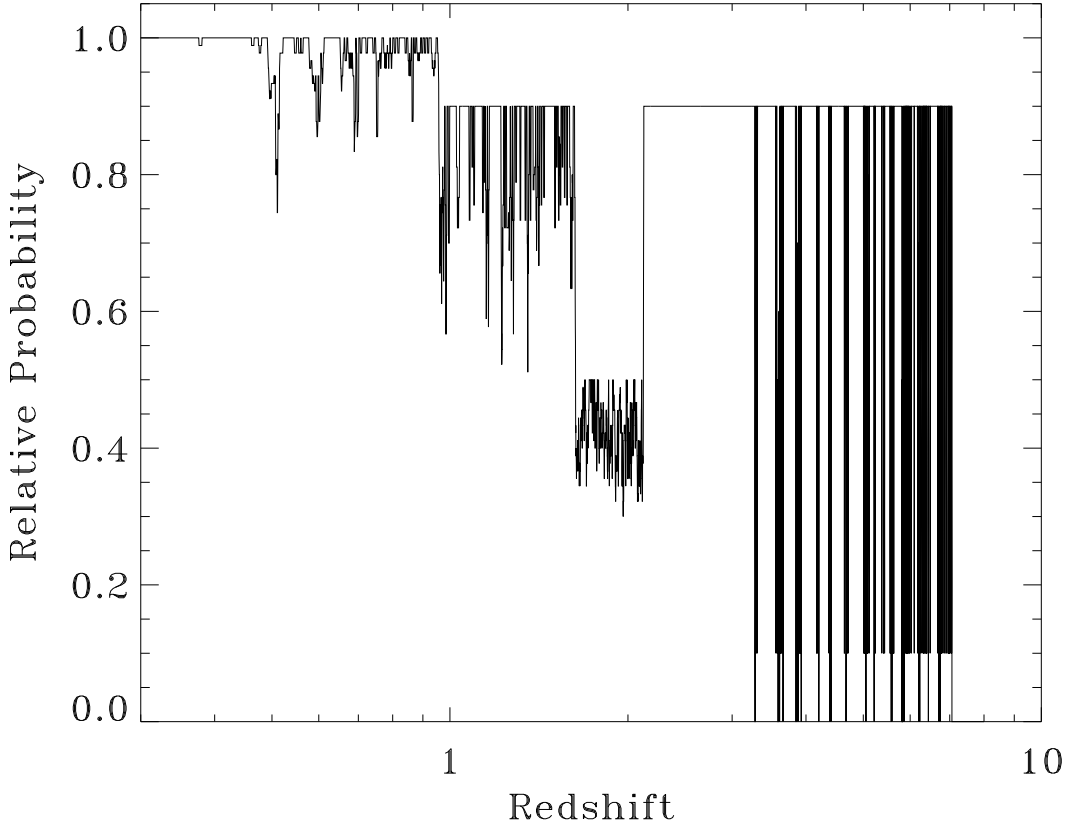


Fig. 3.— A toy model for the redshift observability with ground-based optical spectroscopy in the presence of sky emission lines,  $P_S(z)$ , for an instrumental resolution of  $5 \text{ \AA}$ . The observability of prominent star-formation emission lines (e.g., Ly  $\alpha$ , [O II]) and gaseous halo absorption lines (e.g., Fe I, Mg II) have been modeled using the wavelengths of bright night sky lines as a mask; see text. The decrement of probability between  $1.5 < z < 2$  is due to the inaccessibility of redshifted Ly $\alpha$ , H $\alpha$ , and [O II]  $\lambda\lambda 3727 \text{ \AA}$  in the optical bandpass. No optical redshift can be determined for bursts beyond  $z \approx 7$ , due to Lyman  $\alpha$  blanketing of the optical spectra. The assignment of relative probability goes as follows: If one prominent emission line is observable, then we set  $P_S(z_0) = 0.9$ . If more than 1 emission line is observable then  $P_S(z_0) = 1.0$ . If no emission lines are observable but at least a few prominent metal absorption lines are observable, then  $P_S(z_0) = 0.3$ . If four of these nine absorption lines are observable then  $P_S(z_0) = 0.4$ ; for five observable lines,  $P_S(z_0) = 0.5$ , etc. The main results of this paper are not strongly sensitive to the precise values of these (arbitrary) probability assignments.

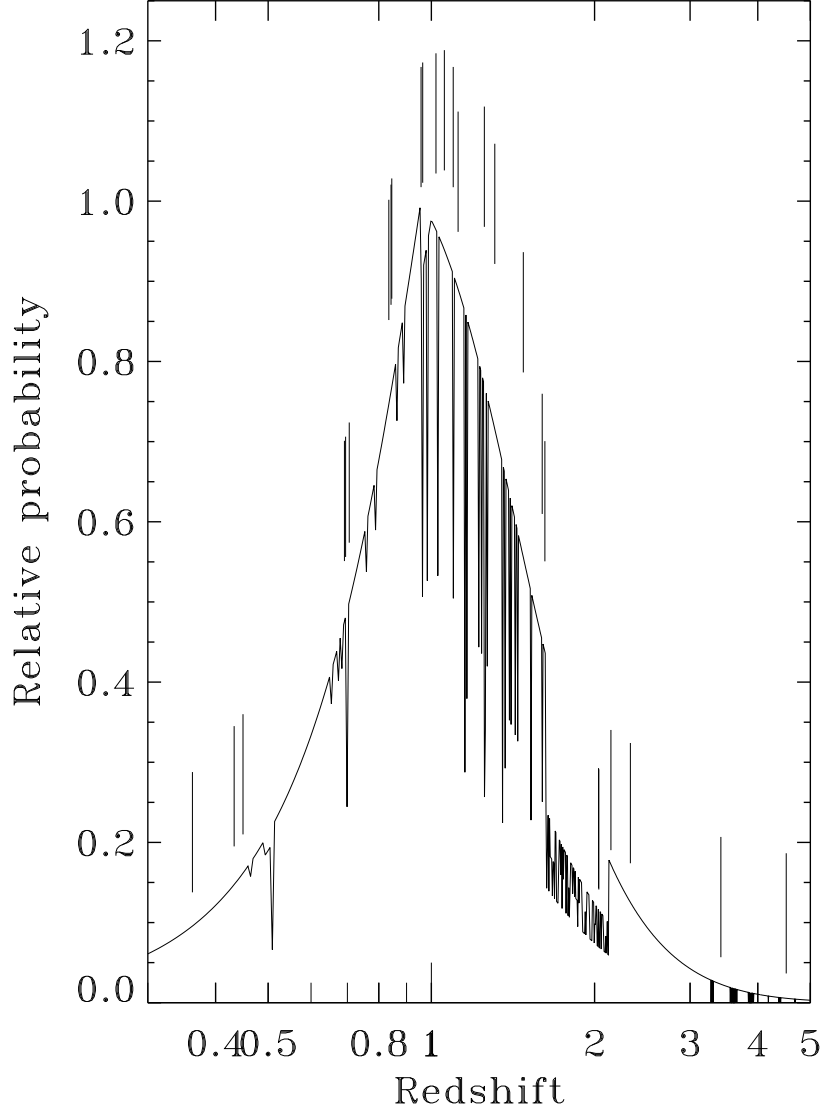


Fig. 4.— A model distribution,  $P(z)$ , of the relative probability for GRB redshift discovery using ground-based optical spectroscopy. The model is shown with low resolution for clarity. The overall shape is determined by the rate density,  $P_G(z)$ , constructed assuming that the GRB rate should follow the Madau star-formation rate (SF1). Beyond redshift of  $z = 1$  we assume that the relative detectability of emission features in GRB hosts, drop as the inverse square of the luminosity distance ( $L = -2$ ). The uncertainty in the precise value of  $L$  (and hence  $P_L(z)$ ) is also confounded by an uncertainty in the correct form of the rate density. The toy model for the redshift observability due to sky-lines is shown in Figure 3. The observed redshifts are noted as vertical lines above the distribution. A machine-readable data file of the high resolution version of this model may be obtained from the author by request.

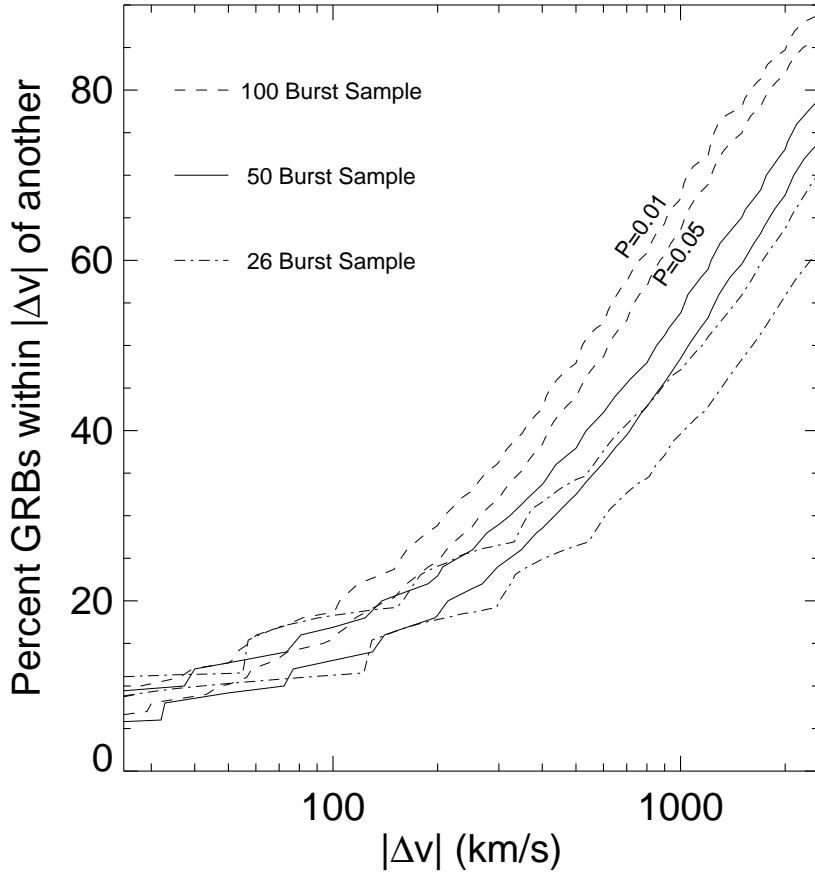


Fig. 5.— Thresholds for the detection of significant small-scale clustering as a function of GRB redshift sample size. Based upon the Monte Carlo simulation (with SF1), the curves show the observed percentage of bursts required to be close to another burst as a function of velocity difference for 95% and 99% confidence. For instance in a sample of 100 ground-based optical redshifts, 66 bursts must lie within 1000 km/s of another burst (i.e., 33 close pairs) to be considered a statistically significant excess. Note that for all samples sizes the percent requirements are similar for small velocity offsets, but diverge at large velocity offsets: with more bursts, the redshift density increases, so random pairing becomes more likely.

Table 1. Measured and corrected GRB redshifts

Burst Name	Pos. (J2000) $\alpha/\delta$	$\theta_{\text{CMB}}$ $^{\circ}$	$v_{\odot, \text{proj}}$ $\text{km s}^{-1}$	redshift type	redshift lines	$z$	$z_{\text{hf}}$	Ref.
011121	11:34:30.4 -76:01:41	69.1	130.0	em	[O II], H $\beta$ , [O III], He I, H $\alpha$	0.362(1)	0.363(1)	1
990712	22:31:53.1 -73:24:28	99.4	-59.4	em/abs	[O II], [Ne III], H $\alpha$ , H $\beta$ , [O III]	0.4331(2)	0.4328(2)	2
010921	22:55:59.9 +40:55:53	145.8	-302.0	em	[O II], H $\beta$ , [O III], H $\alpha$	0.4509(4)	0.4494(4)	3
020405	13:58:3.1 -31:22:22	45.6	255.5	em	[O II], [Ne III], H $\beta$ , H $\gamma$ , [O III]	0.68986(4)	0.69130(8)	4
970228	05:01:46.7 +11:46:54	94.1	-26.3	em	[O II], [Ne III]	0.6950(3)	0.6949(3)	5
991208	16:33:53.5 +46:27:21	88.4	10.2	em	[O II], [O III]	0.7055(5)	0.7056(5)	6
970508	06:53:49.5 +79:16:20	92.3	-14.7	em/abs	[O II], [Ne III]	0.8349(3)	0.8348(3)	7
990705	05:09:54.5 -72:07:53	83.6	40.6	em	[O II]	0.8424(2)	0.8426(2)	8
000210	01:59:15.6 -40:39:33	119.0	-176.8	em	[O II]	0.8463(2)	0.8452(2)	9
970828	18:08:34.2 +59:18:52	103.1	-82.5	em	[O II], [Ne III]	0.9578(1)	0.9573(1)	10
980703	23:59:6.7 +08:35:07	168.4	-357.6	em/abs	[O II], H $\delta$ , H $\beta$ , H $\gamma$ , [O III]	0.9662(2)	0.9639(2)	11
991216	05:09:31.2 +11:17:07	92.2	-14.0	em/abs	[O II], [Ne III]	1.02(2)	1.02(1)	12
000911	02:18:33.2 +07:45:48	134.0	-253.5	em	[O II]	1.0585(1)	1.0568(1)	13
980613	10:17:57.6 +71:27:26	78.9	70.0	em	[O II], [Ne III]	1.0969(2)	1.0974(2)	14
000418	12:25:19.3 +20:06:11	32.4	308.2	em	[O II], He I, [Ne III]	1.1181(1)	1.1203(1)	15
020813	19:46:41.9 -19:36:05	122.7	-197.3	abs	Si II, C IV, Fe II, Al II, Al III, Mg I, Mg II, Mn II	1.254(2)	1.253(2)	16
990506	11:54:50.1 -26:40:35	22.1	338.2	em	[O II] (resolved)	1.306576(42)	1.309180(135)	15
010222	14:52:12.6 +43:01:06	70.4	122.4	abs	Si II, C IV, Fe II, Al II, Sn II, Mg I, Mg II, Mn II	1.4768(2)	1.4778(2)	17
990123	15:25:30.3 +44:45:59	76.5	85.1	abs	Al III, Zn II, Cr II, Zn II, Fe II, Mg II, Mg I	1.6004(8)	1.6011(8)	18
990510	13:38:7.7 -80:29:49	75.4	91.9	abs	Al III, Cr II, Fe II, Mg II, Mg I	1.6187(15)	1.6195(15)	2
000301C	16:20:18.6 +29:26:36	82.1	50.1	em/abs	Fe II, Mg II, O I, C II, Si IV, Si II, C IV, Fe II, Al II	2.0335(3)	2.0340(3)	19
000926	17:04:9.8 +51:47:11	94.1	-26.2	abs	Si II, C IV, Al II, Si II, Al III, Zn II, Fe II, Mg II, Mg I	2.0369(6)	2.0366(7)	20
011211	11:15:18.0 -21:56:56	15.0	352.6	abs	Si II, Si IV, Cr II, Cr II, Si II, C IV, Al II, Fe III	2.140(1)	2.144(1)	21
021004	00:26:54.7 +18:55:41	158.4	-339.4	em	Ly $\alpha$	2.332(1)	2.328(1)	22
971214	11:56:26.0 +65:12:00	72.6	109.1	em	Ly $\alpha$	3.42(1)	3.42(1)	23
000131	06:13:31.0 -51:56:40	75.2	93.2	abs	Lyman $\alpha$ forest	4.511(2)	4.513(2)	24

Note. — Column (5) gives the method of redshift determination for the burst (em = emission-line, abs = absorption-line) and column (6) lists the specific atomic species used to measure the redshift given in column (7). The redshift, corrected to the local Hubble frame, is given in column (8), following from equation 1.

References. — 1. Garnavich et al. (2003); 2. Vreeswijk et al. (2001); 3. Price et al. (2002b); 4. Price et al. (2002c); 5. Bloom et al. (2001); 6. Djorgovski et al. (1999); 7. Bloom et al. (1998); 8. Le Floch et al. (2002); 9. Piro et al. (2002); 10. Djorgovski et al. (2001a); 11. Djorgovski et al. (1998); 12. Vreeswijk et al. (1999); 13. Price et al. (2002a); 14. Djorgovski et al. (2000); 15. Bloom et al. (2003); 16. Barth et al. (2003); 17. Castro et al. (2001); 18. Kulkarni et al. (1999); 19. Castro et al. (2000a); 20. Castro et al. (2000b); 21. Holland et al. (2002); 22. Matheson et al. (2002); 23. Kulkarni et al. (1998); 24. Andersen et al. (2000)

Table 2. Nearest GRB neighbors in redshift and velocity space

Burst Name	$z_{\text{hf}}$	Nearest Burst Name	$\Delta\Theta$ °	$ \Delta z $	$ \Delta v $ km s <sup>-1</sup>
GRB 011121	0.363(1)	GRB 990712	30.3	0.070(1)	15053 ± 223
GRB 990712	0.4328(2)	GRB 010921	114.4	0.0166(4)	3457 ± 93
GRB 010921	0.4494(4)	GRB 990712	114.4	0.0166(4)	3457 ± 93
GRB 020405	0.69130(8)	GRB 970228	133.4	0.0036(3)	628 ± 55
GRB 970228	0.6949(3)	GRB 020405	133.4	0.0036(3)	628 ± 55
GRB 991208	0.7056(5)	GRB 970228	121.4	0.0107(5)	1887 ± 102
GRB 970508	0.8348(3)	GRB 990705	152.1	0.0078(3)	1278 ± 59
GRB 990705	0.8426(2)	GRB 000210	39.0	0.0026(2)	416 ± 47
GRB 000210	0.8452(2)	GRB 990705	39.0	0.0026(2)	416 ± 47
GRB 970828	0.9573(1)	GRB 980703	81.4	0.0066(2)	1008 ± 38
GRB 980703	0.9639(2)	GRB 970828	81.4	0.0066(2)	1008 ± 38
GRB 991216	1.02(1)	GRB 000911	42.3	0.04(1)	5419 ± 2967
GRB 000911	1.0568(1)	GRB 991216	42.3	0.04(1)	5419 ± 2967
GRB 980613	1.0974(2)	GRB 000418	54.6	0.0229(2)	3253 ± 35
GRB 000418	1.1203(1)	GRB 980613	54.6	0.0229(2)	3253 ± 35
GRB 020813	1.253(2)	GRB 990506	104.1	0.057(2)	7446 ± 266
GRB 990506	1.309180(135)	GRB 020813	104.1	0.057(2)	7446 ± 266
GRB 010222	1.4778(2)	GRB 990123	6.2	0.1233(8)	14550 ± 95
GRB 990123	1.6011(8)	GRB 990510	126.2	0.0184(17)	2109 ± 195
GRB 990510	1.6195(15)	GRB 990123	126.2	0.0184(17)	2109 ± 195
GRB 000301C	2.0340(3)	GRB 000926	23.8	0.0026(7)	259 ± 75
GRB 000926	2.0366(7)	GRB 000301C	23.8	0.0026(7)	259 ± 75
GRB 011211	2.144(1)	GRB 000926	105.4	0.107(1)	10383 ± 119
GRB 021004	2.328(1)	GRB 011211	163.0	0.185(1)	17082 ± 132
GRB 971214	3.42(1)	GRB 000131	134.1	1.09(1)	65197 ± 654
GRB 000131	4.513(2)	GRB 971214	134.1	1.09(1)	65197 ± 654

Table 3. Testing the Significance of the Observed Small-scale Structure

$ \Delta v $ km s <sup>-1</sup>	# GRBs paired $\leq  \Delta v $	Prob. (Observed Simulation, $L = -2$ )			Simple Prob.
		$P_G(z) \propto \text{SF1}$	$\propto \text{SF2}$	$\propto \text{SF3}$	
259	2	0.530	0.471	0.438	0.408
416	4	0.303	0.247	0.215	0.252
628	6	0.206	0.145	0.120	0.191
1008	8	0.187	0.126	0.096	0.171
1278	9	0.192	0.120	0.088	0.160
1997	10	0.402	0.275	0.213	0.110
2109	12	0.225	0.133	0.093	0.099
3253	14	0.373	0.222	0.159	0.034
3457	16	0.199	0.092	0.060	0.026
5419	18	0.364	0.199	0.135	0.002
7446	20	0.401	0.230	0.165	6e-5

Note. — Columns (3)–(6) give the probability estimates of observing, by random chance, at least the observed number of GRBs (column 2) that are paired with another within a velocity of  $|\Delta v|$  (column 1). Columns (3)–(5) give the results from the Monte Carlo simulations described in the text for different functional forms of the universal star-formation rate. The last column gives the simplistic probability calculation of observing *exactly* the number of pairs assuming uniform selection in velocity space (equation 4 with  $k = \text{col. [2]}/2$ ). The approximation breaks down for large velocities because the probabilities of observing *more* than the given number of bursts becomes non-negligible and relativistic velocity subtraction is not taken in to account.